Journal of Research in Pharmacy

Research Article

www.jrespharm.com

Development of biosynthesized silver nanoparticles from *Cinnamomum tamala* for anti-oxidant, anti-microbial and anti-cancer activity

Laxman S VIJAPUR*[1], Y. SRINIVAS[2], Anita R DESAI[1], Avinash S GUDIGENNAVAR[1], Somalingesh L SHIDRAMSHETTAR[1], Pooja YARAGATTIMATH[1]

1 Department of Pharmaceutics, Faculty of BVVS Hanagal Shri Kumareshwar College of Pharmacy, Bagalkot, RGUHS Bengaluru, India.
2 Department of Pharmacognosy, Faculty of BVVS Hanagal Shri Kumareshwar College of Pharmacy, Bagalkot, RGUHS Bengaluru, India.
* Corresponding Author. E-mail: laxman906@yahoo.co.in (L.V.); Tel. +919035608179

Received: 08 September 2022 / Revised: 17 October 2022 / Accepted: 21 October 2022

ABSTRACT: **Purpose:** The purpose of this study was to determine the effect of biosynthesized silver nanoparticles (AgNPs) from *Cinnamomum tamala* aqueous extract (CTAE) for antioxidant, antimicrobial and anticancer activity.
Experimental approach: Biosynthesis of AgNPs was successfully achieved by using CTAE by eco-friendly and a cheaper method. In this study we used CTAE for biosynthesis, which reduces silver ions into AgNPs. The obtained AgNPs were characterized by UV, FTIR, DLS, TEM and EDAX analysis. They were further analyzed for their anti-oxidant, anti-microbial, anti-cancer activities.
Key results: The presence of biosynthesized AgNPs (422nm) was confirmed by UV-visible spectroscopy. FT-IR spectrum was used to confirm the presence of different functional groups in the biomolecules which were responsible for capping & reducing of the nanoparticles. Dynamic light scattering of the prepared formulations revealed all the formulations were in nano- range, F1 showed the mean particle size 239.1nm.TEM Analysis revealed that the size of the particleswere in nano-range of 20.38nm and presence of silver was confirmed through EDAX. The IC50 value of F1 indicated 91.30µg/ml for H_2O_2 scavenging activity and 102.43µg/ml for DPPH scavenging activity. Biosynthesized AgNPs (F1) showed good antimicrobial activity against two gram negative bacteria and one gram positive bacteria. MTT assay of optimized formulation F1 was compared with CTAE showed significant antiproliferative activity against A375 cancer cell line with IC50 for CTAE was 47.24µg/ml, where as for biosynthesized AgNPs the IC50 was 22µg/ml. Apoptosis studies of formulation F1 showed higher early apoptosis as compared to CTAE.
Conclusion: The biosynthesized silver nanoparticles (F1) showed good antioxidant activity, antimicrobial activity and anti cancer activity compared to CTAE.

KEYWORDS: *Cinnamomum tamala;* Silver nitrate; Silver nanoparticles; Anticancer activity; Anti-microbial activity; Anti-oxidant activity

1. INTRODUCTION

The proper management of microbial illnesses is now under risk due to the emergence of drug-resistant bacteria. The sensitivity of microorganisms to these drugs has increased despite the pharmaceutical industry's manufacture of various new antibiotics because infections have the genetic ability to evolve and disseminate resistance to synthetic medicines that are being utilised as therapeutic agents. The emergence of multiple drug resistance has made it difficult to generate new synthetic antimicrobial drugs, necessitating the discovery for inventive antimicrobials derived from natural plant sources[1].

The body in stress produces free radicals, which are important for many routine cellular processes. High quantities of free radicals may harm the body and damage cell organs, including DNA, proteins, and cell membranes, which may hasten the development of cancer and other disorders. Free radicals are neutralised by antioxidants, which also stop cell damage[2]. Cell proliferation, angiogenesis, and metastasis are three processes that contribute to the progression of cancer and are influenced by a variety of pathogenic and metabolic alterations in the cellular environment. Cancer cells have aberrant metabolic -functions include aerobic glycolysis, mitochondrial DNA destruction, changes to the respiratory chain, and altered gene

How to cite this article: Vijapur LS, Srinivas Y, Desai AR, Gudigennavar AS, Shidramshettar SL, Yaragattimath P. Development of biosynthesized silver nanoparticles from *Cinnamomum tamala* for anti-oxidant, anti-microbial and anti-cancer activity. J Res Pharm. 2023; 27(2): 769-782.

ISSN: 2630-6344
http://dx.doi.org/10.29228/jrp.359

expression[3,4]. In humans, the skin is the largest organ, accounting for 15% of the typical adult's total weight. Given that it is made up of several tissue types and has heterogeneous embryological origins, it is regarded as a complicated organ (ectodermal and mesodermal). The fundamental functions of the skin include the body's defence against external impacts, regulation of body temperature, maintenance of fluid and electrolyte balance, endocrine and exocrine activity, perception of stimuli, and generation of vitamin D, among other things[5].

Skin cancer falls into two categories: melanoma and non-melanoma. UVR exposure has been related to a range of negative effects, including skin cancer. UVR wavebands exhibit diverse cellular and molecular changes. The generation of ROS by cellular chromophores as a result of UVA radiation-induced photosensitization is linked to inflammation and photoaging of exposed skin and is thought to be the origin of these effects[6]. Cytotoxicity refers to how much exposure to nanoparticles alters the cellular processes and structures necessary for cell survival and growth. Utilizing cytotoxicity assays, first assessments of acute toxicity may be made fast and easily. By integrating data from cytotoxicity tests with data from other safety testing, one may predict the biocompatibility of nanoparticles. Their cytotoxicity refers to the extent to which cellular processes and structures necessary for cell survival and proliferation are changed as a result of interaction with nanoparticles. Cytotoxicity assays can be used to do initial assessments of acute toxicity fast and easily. Data from cytotoxicity tests and data from other safety studies can be used to predict the biocompatibility of nanoparticles. Recent years have seen an enormous increase in research on the cytotoxicity of AgNPs on a variety of cancer cell lines, including those used to study skin cancers of the melanoma type. This has led to the inclusion of AgNPs as one of the new therapeutic options with potential for the treatment of this type of topical lesions[5].

The term "nanotechnology" refers to the study of materials with a scale smaller than 100 nanometers, as well as the design, production, assembly, and characterization of these materials, as well as the use of miniature functional systems derived from these materials in biology, chemistry, physics, food, medicine, electronics, aerospace, medicine, and other fields. Among various metal nanoparticles, biologically synthesized silver nanoparticles are one of the promising candidates in biomedical research due to the presence of their unusual physiochemical properties, tunable size and shape, ease of synthesis and characterizations, and biocompatibility. While the majority are classified as silver due to their high surface to bulk silver atom ratio, some are made up mostly of silver oxide. Depending on their intended application, nanoparticles can take on a variety of forms. Additionally, silver has been used extensively as a medicinal agent for the treatment of various diseases since ancient times. Furthermore, the active molecules from biological sources potentiate the overall therapeutic effect of biosynthesized silver nanoparticles[7]. Silver nanoparticles made physically or chemically provide a major risk to the environment and human health. The creation of nanoparticles using plant and bacterial extracts has lately gained popularity as a "green synthesis" method that may solve the problem of toxicity imposed by physical and chemical procedures.Several plants, including *Punica granatum*[8], *Piper nigrum Concoction*[9], *Rosa damascene* [10], and *Cleome viscosa* L[11], have been used in studies of green production of silver nanoparticles for their increased anti-cancer action.

The components of *Cinnamomum tamala* leaves exhibited antitumor action against human ovarian cancer cells. Bornyl acetate, found in its leaf extract, has a potent *in-vitro* cytotoxic effect on cancer cells. It improves hyperplastic changes and considerably lowers prostatic hypertrophy. It could reduce cancer cell viability, halt the cell cycle, cause apoptosis, oxidative stress, and DNA damage[12,13].India is a country located in tropical region with an abundance of natural resources. Given their lack of toxins and environmental safety, plants are the best production platform for nanoparticles. Plants have a wide range of biomolecules with different functional groups which help to reduce & cap silver ions to AgNPs. As significant phytochemical components of *Cinnamomum tamala* are tannins, alkaloids, flavonoids, and terpenoids have demonstrated therapeutic usefulness[14].Eugenol (4-hydroxy-3-methoxyallylbenzene) is the main component in cinnamon oil, followed by ß-caryophyllene (6.6%), sabinene (4.8%), germacrene D (4.6%), and curcumenol (2.3%). Camphene, myrcene, limonene, methyl ethyl eugenol, and alfapinene are among the chemical components of bay leaves that are most prevalent. *Cinnamomum tamala* also known as Indian bay leaf, or Tejpat, is a member of the Lauraceae family. It is a medium-sized evergreen tree that is frequently used to flavour food. Additionally, due to its wide usage in pharmaceutical manufacture and its pharmacological capabilities, such as antioxidant[2], and antimicrobial[15], it has many medicinal uses. Due to the perfume and flavour of the leaves, which contain an essential oil, *Cinnamonomum tamala* is frequently used as a spice in Indian cuisine[16].

Howerever, up till now, the effect of silver nanoparticles of *Cinnamomum tamala* extract on improvement of anti-oxidant, anti-microbial and anticancer activity on A375 cell lines has not been investigate.

The current study examined the anti-oxidant, anti-microbial and anticancer properties of CTAE and biosynthesized silver nanoparticles.

2. RESULTS

2.1. UV-Spectroscopy of CTAE and AgNPs

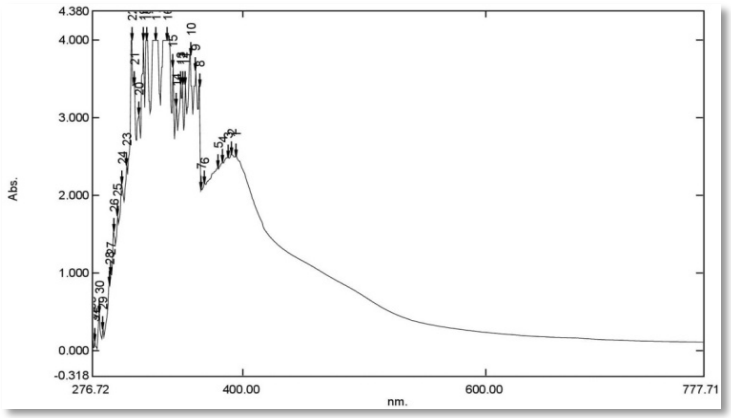

Figure 1a. UV-Spectroscopy of CTAE

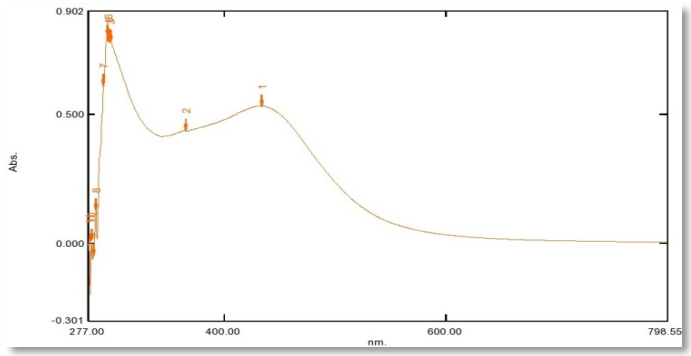

Figure 1b. Uv-spectroscopy of AgNPs

2.2. FT-IR Spectroscopy of CTAE and AgNPs

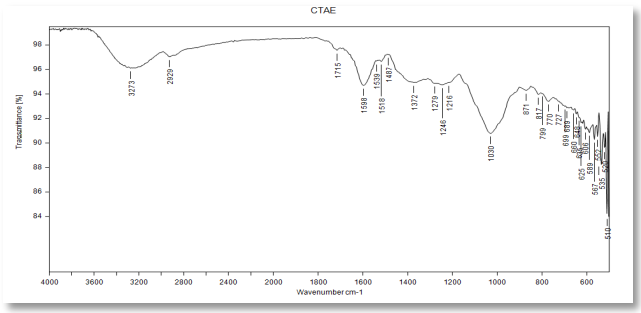

Figure 2a. FT-IR spectroscopy of CTAE

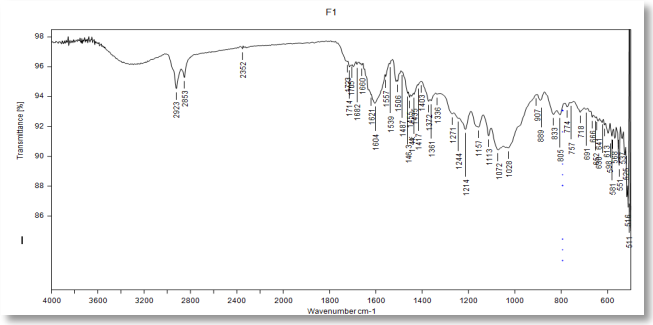

Figure 2b. FT-IR spectroscopy of AgNPs

2.3. Transmission electron spectroscopy (TEM) and EDAX

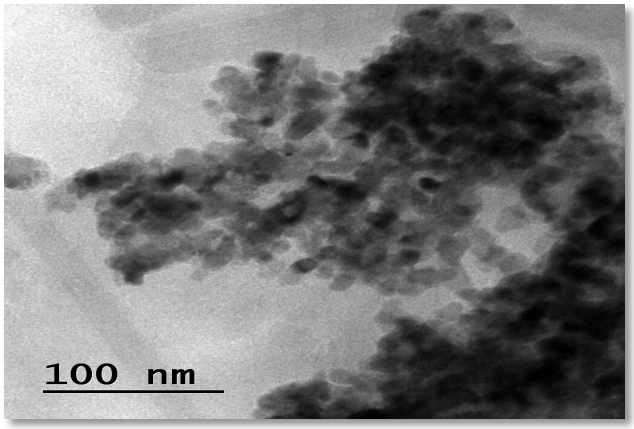

Figure 3a. TEM image of AgNPs(F1)

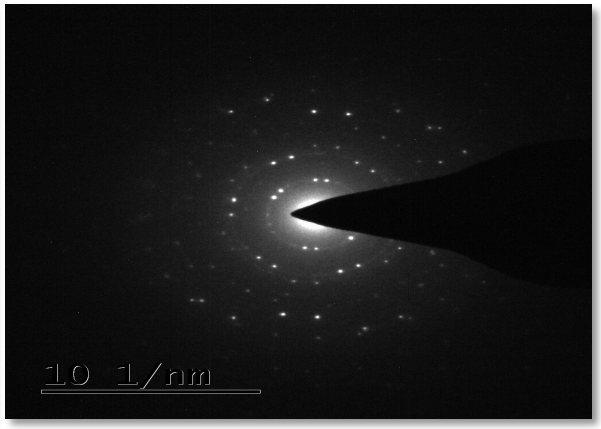

Figure 3b. SAED pattern of AgNPs (F1)

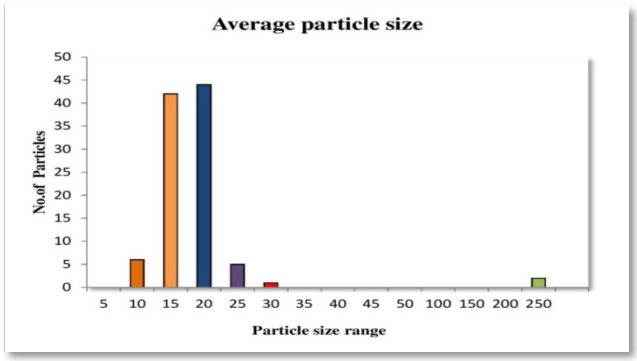

Fig3c.Particle size distribution

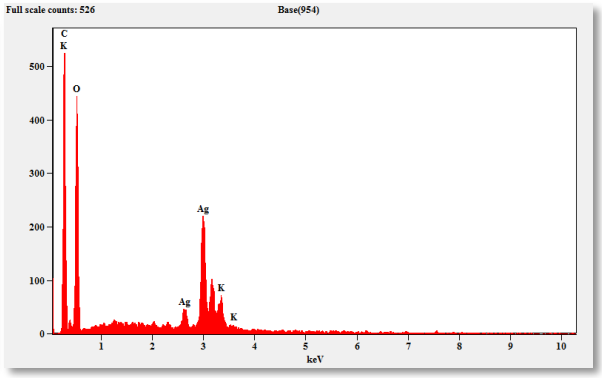

Fig3d. EDAX analysis

2.4. Anti-oxidant activity

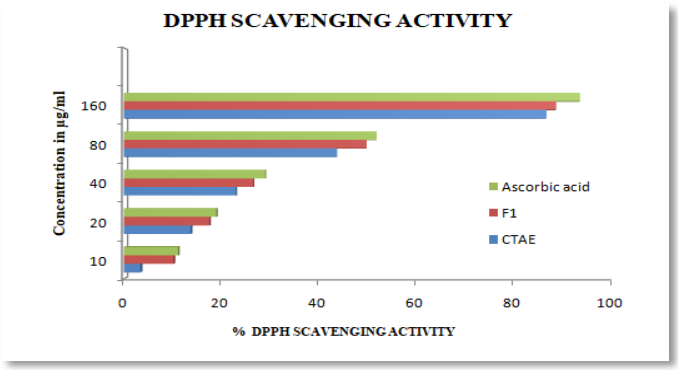

Figure 4a. DPPH scavenging activity

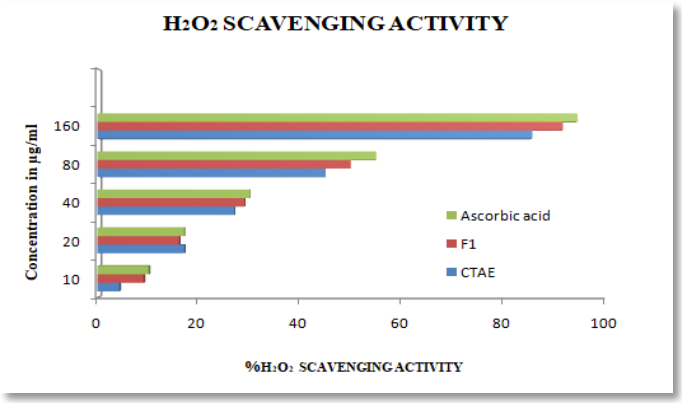

Figure 4b. H_2O_2 scavenging activity

2.5. Anti-microbial activity

SL.No.	Name of Microorganisms	Zone of inhibition(mm)	
		CTAE	F1
1	*E.coli*	R	25mm
2	*Klebsiella*	15mm	09mm
3	*E.fecalis*	R	R
4	*S.mutans*	20mm	13mm

R-Resistance

Table 1. Values of zone of inhibition obtained by disc diffusion method

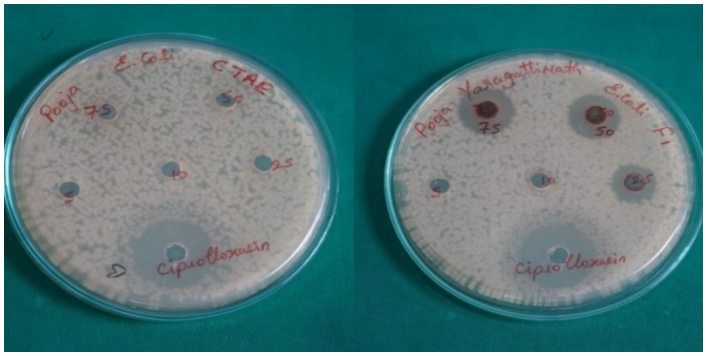

Figure 5a. *E.coli*

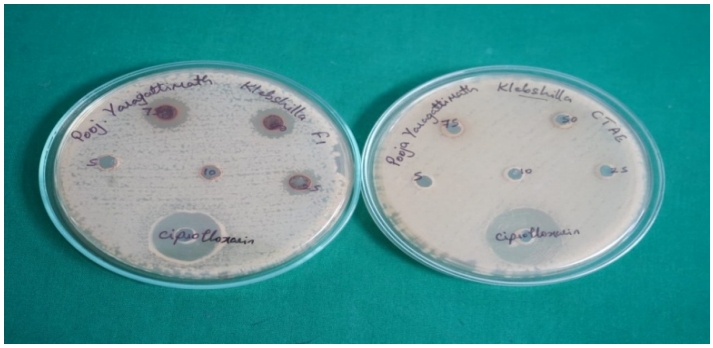

Figure 5b. *Klebsiella*

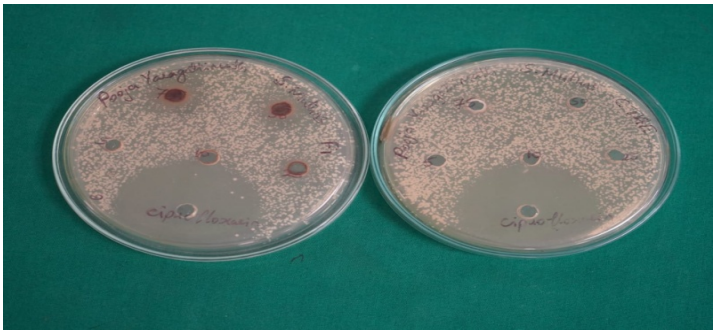

Figure 5c. *S.mutans*

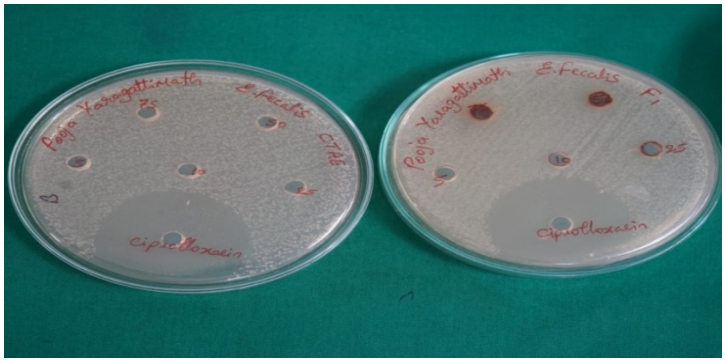

Figure 5d. *E.fecalis*

2.6. Anti-cancer activity

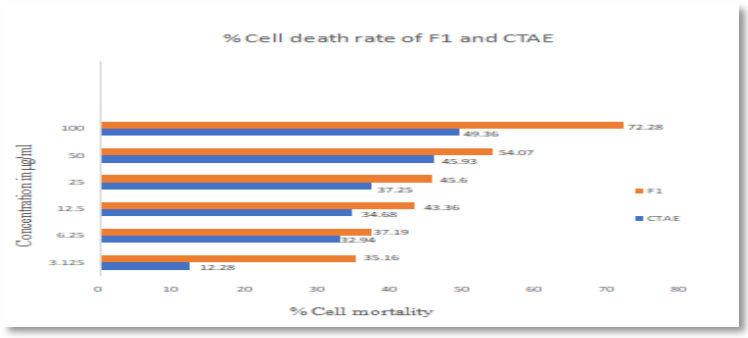

Figure 6a. Percentage cell mortality of Biosynthesized AgNPs (F1) and CTAE

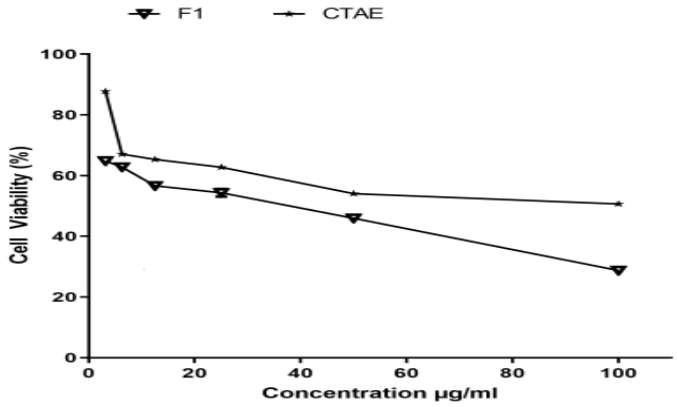

Figure 6b. Percentage viability of A375 cell line vs AgNPs and CTAE

2.7. Flow cytometer analysis

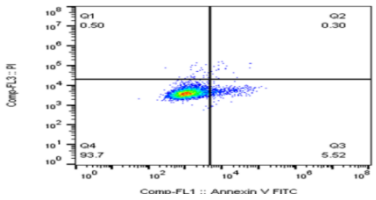

Figure 7a. Control

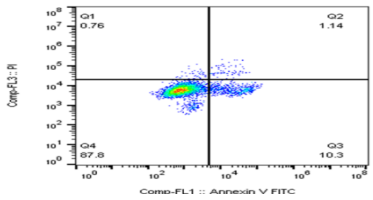

Figure 7b. CTAE

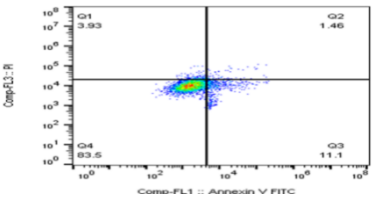

Figure 7c. AgNPs (F1)

3. DISCUSSION

3.1. Phytochemical investigation

Phytochemical investigation of CTAE found to contain Alkaloids, glycosides, flavonoids, steroids and phenolic compounds.

3.2. UV-spectroscopy

The formation and nuclation of AgNPs were monitored UV–visible spectroscopy. To validate the nucleation of AgNPs a UV–Vis spectrophotometer was utilized. The confirmation of silver nanoparticles synthesis was monitored by UV–Vis spectrophotometer as it is the most convenient tool for measuring the reduction of metalic ions. The color shift of the CTAE/silvernitrate combination is recorded visually. Due to the generation of plasmons at the colloid surface, the solution color changed to light yellow after 3 hours, then

to yellowish-brown, indicating that silver nanoparticles are being biosynthesized. The spectra recorded before addition of silver nitrate & after addition of silver nitrate (3hrs) observed increased intensity in absorption spectra of silver solution with time, indicating the formation of increased number of silver nanoparticles in the solution[17].Surface plasmon resonance (SPR) is produced at the nanoparticle interface by incident light-stimulated resonant oscillations of conduction electrons. Metallic Nanoparticles exhibit different optical absorption spectra as a result of this [18]. The UV-Vis absorption spectra of CTAE are shown in Figure 1a and AgNPs from CTAE are shown in Figure 1b after 3 hours. UV–visible spectra revealed a significant band absorption peak at 422 nm (Figure 1b) due to stimulation of the strong band (SPR) As a result, the nanoparticles were isotopic and homogenous in size. The silver nanoparticles absorption spectra were measured against silver nitrate, to study silver nanoparticle production and stability. Spherical nanoparticles produce a single surface plasmon resonance band in absorption spectra, as predicted by Mie's theory. The reaction mixture in this investigation validates single SPR bands revealing that silver nanoparticles in spherical form[19].

3.3. FT-IR spectroscopy

The potential biomolecules involved in silver nanoparticle reduction, capping, and effective stability are determined using Fourier transform infrared spectroscopy. The bio-reduction of Ag+ ions could have been aided by several functional groups present[20]. The band strengths of plant extract and silver nanoparticles in different parts of the spectrum were investigated and are presented in Figure 2a and Figure 2b. The FT-IR spectrum of CTAE has significant peak positions of 3273, 2929, 1715, and 1598 cm^{-1}, while the FT-IR spectra of F1 biosynthesized SNPs have major peak positions of 2923,2853, 1714, and 1604 cm^{-1}.The strong,broad –OH stretching present in CTAE but it is completely capped by silver in F1 bio synthesized SNPs.The FT-IR spectrum of biosynthesized silver nanoparticles shows different peak positions at 1028, 1214, 1244, and 1271cm^{-1}, indicating -C-N stretching vibrations of amine, -C-O-C,or -C-O these absorbance bands have weak intensity and groups like Alkaloids, steroids, and glycosides are present in the extract and function as capping ligands for nanoparticles. The C-H stretch aliphatic can be attributed to 2923 cm^{-1} this band has strong intensity. The weak intensity of 2853cm^{-1} new peak arrives can be assessed as absorption band C-H stretching. At 1714 cm^{-1} the stretching vibration of the carbonyl group -C=O can be seen as the peak intensity is increased. Strong intensity of 1604 cm-1 indicates the presence of a C=C Stretching cyclic alkene in the extract. The vibration of -NO3 stretching was seen at 1372 cm-1. The observed peaks are may be due to the presence of various secondary metabolites in plant extracts, such as flavonoids, triterpenes, tannins, steroids, and saponins may be responsible for the bioreduction.

3.4. Particle size (DLS) and Zeta potential

By detecting dynamic changes in light scattering intensity generated by the Brownian motion of the particles, the size distribution of the particles may be determined. The measurements yielded the average hydrodynamic diameter of the particles, the hydrodynamic diameter distributions peak values, and the polydispersity index (PDI), which defined the particle size distributions breadth[21].The particle size distribution of silver nanoparticles of F1 showed particle size of 239.1nm, F2 showed particle size of 367.7nm, F3 showed particle size of 419.1nm, F4 showed particle size of 1011.9nm, and F5 showed particle size of 1111.5nm. F1 was chosen for further characterization & biological evaluation because it had the lowest particle size of 239.1nm, which will be having highest surface area due to this F1 may show good anti-oxidant, anti-microbial and anti-cancer activity.

3.5. Transmission electron microscopy and EDAX

The size and form of the resultant particles were determined using TEM. Aliquots of F1 biosynthesized SNPs solution were sprayed over a carbon-coated copper grid and allowed to dry at room temperature. A TEM image was captured, well. The TEM found that the size detected was smaller than the DLS analysis [22], this is due to DLS measures hydrodynamic size where as TEM measures actual diameter. According to the TEM images Figure 3a shows the generated silver nanoparticles were generally spherical and polydisperse in form and AgNPs were layered by a faint thin layer of other material, which is believed to be capping of organic material from the CTAE. TEM image with a selected area electron diffraction (SAED) pattern is also shown in Figure 3b. The average particle size of the nanoparticles seen in the TEM images was confirmed using ImageJ version 1.4.3.67 software. The particles were analyzed, and a histogram was generated by adding numbers in Excel software to calculate the average particle size shown in Figure 3c, which was about 20.38nm. The EDAX spectrum revealed the purity and the complete chemical composition of AgNPs. The percentage of Ag metal found in occurrence with other chemical elements was found to be percentage.

The reduced silver nanoparticles were subjected to EDAX analysis showed strong peak at 3 keV. The EDAX analysis showed percentage of silver (Ag) was 26.44%.

3.6. Anti-oxidant activity

DPPH scavenging activity

The DPPH scavenging activity technique was used to test the antioxidant activity of biosynthesized AgNPs and CTAE. The decrease of DPPH free radical activity is dependent on the reduction of DPPH is converted to DPPH-H, which is a hydrogen-donating antioxidant**.** The *in-vitro* antioxidant activity results showed that the antioxidant DPPH scavenging activity increased with the increase in the concentration. (10µg/ml, 20µg/ml, 40µg/ml, 80µg/ml, 160µg/ml) of the biosynthesized AgNPs(F1), CTAE and ascorbic acid was used as standard. The percentage of DPPH scavenging activity results of the biosynthesized AgNPs shown in Figure 4a.The IC_{50} values were observed as 84.34µg/ml of AgNPs (F1), 91.02µg/ml of CTAE, and 79.41 µg/ml of Ascorbic acid. Therefore, it was concluded that the biosynthesized AgNPs (F1) showed very good DPPH scavenging activity when compared to the CTAE.

H_2O_2 scavenging activity

The production of hydrogen peroxide in live cells causes a rise in reactive oxygen species (ROS) such as hydroxyl and peroxides, which cause severe cell membrane damage. On the test samples, the hydrogen peroxide free radical scavenging ability was tested. The *in-vitro* antioxidant activity results Figure 4b showed that the antioxidant Hydrogen peroxide scavenging activity increased with the increase in the concentration. (10µg/ml, 20µg/ml,40µg/ml,80µg/ml,160µg/ml) of the test samples i.e., the biosynthesized AgNPs(F1), CTAE and ascorbic acid used as standard. The percentage of hydrogen peroxide scavenging activity results of the biosynthesized AgNPs shown in Figure 7b. The IC_{50} values were observed as 82.25µg/ml of AgNPs (F1), 89.52µg/ml of CTAE, and 78.12 µg/ml of Ascorbic acid [23].

When compared to the IC50 values of DPPH scavenging activity and H_2O_2 scavenging activity, the H_2O_2 scavenging activity's result was good. Due to the presence of bioactive molecules on the surface of silver nanoparticles.

3.7. Anti-microbial activity

Silver nanoparticles may adhere to the cell membrane's surface and impair vital processes including permeability and respiration. It makes sense to say that the amount of surface area available for contact determines how tightly the particles are bound to the bacterium. Smaller particles will have a greater bactericidal impact than bigger ones because they have a wider surface area for contact[24]. Antimicrobial tests were conducted in the current study on two gram negative bacteria, *E. coli* and *Klebsilla*, and two gram positive bacteria, *Streptococcus mutans* and *E. fecalis*. In our study, F1 and CTAE were tested for their antimicrobial efficacy and were found effective against gram negative and gram positive bacteria shown in Table no 1. The F1 showed their good anti-microbial activity against *E.coli*(gram negative bacteria) with showed zone of inhibition measuring 25mm.

3.8. MTT assay

Melanoma is the most lethal and life-threatening form of skin cancer, with increasing rates of occurrence across the world. Exposure of the skin to dissimilar external factors, mainly solar radiation,its cells are prone to alterations in their reproductive cycle and frequently generate changes in cell division processes associated with proliferative processes that trigger some type of skin cancer[8].UV radiation can damage DNA and thus mutagenize several genes involved in the development of skin cancer. The presence of typical signature of UV-induced mutations on these genes indicates that the ultraviolet-B part of cutaneous carcinogenesis[9]. The cytotoxicity of green synthesized AgNPs was investigated using the MTT test in this work, and it was found that F1 have anti-cancer action against A375 human melanoma cell lines. At a concentration of 3.125µg/ml to 100µg/ml Cell mortality was found to be increased when the quantity of CTAE and AgNPs was increased, as shown in Figure 6a. The IC50 of CTAE on the A375 Melanoma cancer cell line was 47.24µg/ml, while the IC50 of biosynthesized AgNPs was 22µg/ml. The results revealed that the cytotoxicity of human A375 melanoma cells was dose-dependent. CTAE had a viability of cells 50.64% at 100µg/ml, whereas synthesized silver nanoparticles (F1) had a viability rate of 28.72% at 100 µg/ml. % Viability of A375 cell line vs CTAE and F1 shown in Figure 6b. This might be owing to the saturation impact of silver nanoparticles at concentrations above 100µg/ml on A375cells. When biosynthesized AgNPs were compared to aqueous extract, they were more death of A375 cells. This might be owing to the alkaloids, glycosides, phenolic compounds, and tannins found in CTAE, which encapsulated silver ions.

3.9. Apoptosis analysis by flow cytometer

Apoptosis is a form of programmed cell death to remove unwanted, damaged cells from tissues. The process of cell death known as apoptosis, which is mediated by a group of enzymes known as caspases, and the apoptosis is morphologically distinct from necrosis. It is a balancing mechanism that allows for a physiological balance of cells and is important for many processes, including embryogenesis, neuronal synaptic connection, the development of the immune response, and the elimination of cancer cells, infected cells, and cells damaged by toxic agents, among others[8].In our present study the staining was carried out in four quadrants: live, early apoptosis, late apoptosis, and dead**.** Flow cytometric photograms of A375 cells after 24 hours of treatment with CTAE and F1 can be shown in Figure 7b and Figure 7c. 93.7 % of untreated cells survived, compared to 87.8% for CTAE and 83.5% for F1 formulation. Early apoptosis was found to be 10.3% for CTAE and 11.1% for AgNPs (F1), while late apoptosis was found to be 1.14% for CTAE, and F1 was 1.46%, and death was found to be 0.76% for CTAE and 3.8% for F1. When compared to CTAE, the findings of apoptosis revealed that F1 had a higher proportion of cells death in early apoptosis, late apoptosis, and overall death percentage.

4. CONCLUSION

The green chemistry approach to the biosynthesis of AgNPs using *Cinnamomum tamala* has several benefits, including being a cost-effective, energy-efficient, and environmentally friendly process that promotes healthier workplaces and communities while safeguarding human health and the environment. It also results in less waste and safer products. The potentially active phytoconstituents involved in the plant-mediated synthesis of nanoparticles are biocompatible for a wide range of biomedical applications. Additionally, the nanoparticles were studied to show their anti-oxidant activity, anti-microbial activity against Gram-positive and Gram-negative bacteria and anti-cancer activity on skin (melanoma) cancer cell lines, which were A375. Thus, this report adds another feature to the medicinal hub plant *Cinnamomum tamala* i.e., its ability to successfully formulate AgNPs, which could be used effectively for their anti-oxidant, anti-microbial and anticancer properties.

5. MATERIALS AND METHODS

5.1. Materials

Cinnamomum tamala leaves were gathered from a local market of Ilakal and authenticated by Prof. M.K. Ganachari, Department of botany at Basaveshwar Science College in Bagalkot. We bought analytical-grade silver nitrate from SDFCL in Mumbai. The investigation was conducted using double-distilled water.

5.2. Preparation of *Cinnamomum tamala* aqueous extract

The leaves were three times rinsed in double-distilled water. The cleaned leaves were air dried in a shaded area at room temperature. The leaves were crushed after drying, and the powder was kept for further use. 100ml of double-distilled water was used to immerse 10 gm of crushed *Cinnamomum tamala* leaves, which were then left to soak for 24 hours and boiled for 15 minutes at 60 °C. Whatmann filter paper grade no. 1 was used to filter the filtrate. After the extract had been passed through muslin cloth. The solution was centrifuged at 5000 rpm for 15 minutes. For later usage, the leaf extract was kept in a coloured amber glass jar at 4 °C.

5.3. Phytochemical screening of *Cinnamomum tamala* aqueous extract

The phytochemical screening for CTAE was done according to the methods described by Khandelwal et al[25].

5.4. Green synthesis of silver nanoparticles

Aqueous extract of *Cinnamomum tamala* and silver nitrate were used for the bioreduction of silver ions. Different concentration of CTAE was used to biosynthesize the AgNPs by using 1ml (F1), 2ml (F2), 3ml (F3), 4ml (F4), 5ml (F5) and volume was made upto 100ml with 1mM $AgNO_3$ in 250ml Erlenmeyer flask and kept in dark place for 3hrs. After keeping them 3 hours in the dark amber glass container, the colour changed from light-yellow to yellowish-brown. The AgNPs dispersion were centrifuged at 10,000 RPM for 15 minutes to yield the green synthesized silver nanoparticles. To remove any unreacted biological components, the pellet was resuspended in double-distilled water and centrifuged three times. After being purified, the

pellets were dried in a hot air oven at 60°C to produce silver nanoparticles, which were subsequently employed in characterization experiments [26].

5.5. UV-Visible spectrophotometer analysis

In the UV–visible range, the silver nanoparticles exhibit distinctive optical absorption spectra. Between 200 and 800 nm of absorbance were measured. As a blank, silver nitrate solution was employed. At room temperature, the AgNPs dispersion was used for the spectroscopic investigations (Shimadzu, Japan) [18].

5.6. Fourier Transmission Infrared Spectroscopy (FTIR)

Before and after the bio-reduction with $AgNO_3$ for dried biomass of CTAE, FT-IR investigations were conducted using Bruker alpha, Germany. The biomass was dried at 60°C to prepare the samples. Potassium bromide (KBr) was used to grind the solid biomass of CTAE and silver nanoparticles into a fine powder. Since KBr is transparent in the IR, a tiny pellet made of this powder was crushed and examined. By putting the pellet in the holder of the Fourier transform infrared (FTIR) spectrophotometer, FTIR spectra were measured. The dried samples FTIR spectrum was captured[27].

5.7. Particle size and zeta potential measurement

Dynamic light scattering was used to calculate the nanoparticles zeta potential and particle size. 10 ml of double-distilled water were mixed with 1 ml of a nanoparticle solution to create the sample. To ensure appropriate mixing, the dispersion mixture was ultrasonically sonicated for 30 seconds. Following that, the sample was put into a glass cuvette. The measurements of the laser light scattering were taken at a fixed angle of 90° [21].

5.8. Transmission Electron microscopy (TEM) and EDAX

TEM was used to analyze the size and form of the resulting particles. A carbon-coated copper grid was covered with aliquots of an AgNPs dispersion, which were then allowed to dry naturally while TEM images were being captured. The sample was further utilized for the analysis, which was run at 200Kv, after drying on the grid. Both qualitative and quantitative analysis were performed using Energy Dispersive X-ray (EDAX) analysis, which allowed for the identification of the types of elements present as well as the proportion of each elements concentration inside the SNPs[22].

5.9. Anti-oxidant activity

DPPH scavenging activity

The free radical scavenging activity of the CTAE and F1 biosynthesized SNPs was evaluated. Briefly, the plant extract was mixed with a 0.1mM of 1,1-Diphenyl-2-picrylhydrazyl (DPPH) ethanol solution, to give final concentrations of 10, 20, 40, 80, and 160µg of extract per ml of DPPH solution. Ascorbic acid was used as standard. After 30 min at room temperature, the absorbance values were recorded at 517 nm and converted into percentage antioxidant activity.

$$\% \text{ DPPH radical scavenging activity} = \frac{Ac-As}{Ac} \times 100$$

H_2O_2 scavenging activity

The ability of CTAE and F1 to scavenge hydrogen peroxide (40mM/L) was prepared in phosphate buffer (pH 7.4). The concentration of hydrogen peroxide was determined by absorption at 230 nm using a spectrophotometer. CTAE and F1 biosynthesized SNPs were dissolved in distilled water then added to hydrogen peroxide and absorbance at 230nm was determined after 10 min against a blank solution containing phosphate buffer without hydrogen peroxide. The different concentrations of CTAE and F1 biosynthesized SNPs were used in the concentration of 10, 20, 40, 80 and 160µg/ml, Ascorbic acid was used as a standard. The percentage of hydrogen peroxide scavenging was calculated as follows [23].

$$\text{Scavenged } H_2O_2\ (\%) = [(Ac - As)/Ai] \times 100$$

5.10. Anti-microbial activity

Antimicrobial activity of CTAE and its biosynthesized silver nanoparticles (F1) were evaluated by disc diffusion test. For the evaluation of antimicrobial activity of CTAE and its biosynthesized silver nanoparticles the tested against Two Gram positive bacteria *Streptococcus mutans* and *Enterococcus faecalis*,& two Gram negative bacteria such as *Escherichia coli* and *Klebsiella pneumonia.* Brain Heart Infusion agar media was used for study. Inocolums of test microorganism turbidity was adjusted to 0.5 McFarland turbidity

standard and fresh culture inoculated on surface of agar plates with sterile cotton swab. Wells were made with a hollow tube, by heating & Pressing it on above inoculated agar plate and removed it immediately by making a well in the plate. Likewise, five wells were made on each plate. Stock solution was Prepared by weighing 10mg of CTAE AND F1 and dissolved it in 1ml of DMSO & wells were loaded with the different concentrations of CTAE and F1(10mg/ml) 75µl, 50µl, 25µl, 10µl and 5µl. Incubate plates within 15 min of compound application for 24 hrs at 37 ^{o}C in incubator[28].

5.11. Anti-cancer activity by MTT assay

The cells were seeded a 96-well flat-bottom micro plate and maintained at 37˚C in 95% humidity and 5% CO_2 for overnight. Different concentration (100, 50, 25, 12.5, 6.25, 3.125µg/ml) of CTAE & F1 biosynthesized SNPs were treated. The cells were incubated for another 48 hours. The wells were washed twice with Phosphate buffered saline (PBS) and 20µL of the (3-[4,5-dimethylthiazol-2-yl]-2,5-diphenyltetrazolium bromide (MTT) staining solution was added to each well and plate was incubated at 37˚C. After 4h, 100µL of DMSO was added to each well to dissolve the formazan crystals, and absorbance was recorded with a 570nm using micro plate reader[29-30].
Formula: Surviving cells% = Mean Optical density of test compound/ Mean OD of negative control ×100
Using graph pad prism version 5.1, we calculated the IC50 values of CTAE & F1 biosynthesized SNPs.

5.12. Apoptosis by flow cytometer

The cells were seeded in a 6-well flat bottom micro plate containing cover slips and maintained at 37˚C in CO_2 incubator for overnight. The IC50 concentrations CTAE & F1 biosynthesized SNPs were treated at 24 hrs. After the incubation, cells were washed with PBS twice. Centrifuge for 5 minutes at 5000 rpm at 4°C. Supernatant layer was discarded and the cell pellet were resuspended in ice-cold 1X Binding Buffer to 1 x 10^6 per ml. Keep tubes on ice. Then add 5 µl of AbFlour 488 Annexin V (Phospholipid binding protein) and 2 µl Propidium iodide (PI) and Mix gently. Keep tubes on ice and incubate for 15 minutes in the dark. Add 400 µl of ice-cold 1X binding buffer and mix gently. Analyze cell preparations within 30 minutes by flowcytometry. Then analysis was done using FlowJo X 10.0.7 software (2) [31-32].

Acknowledgements: The authors would like to thank Maratha Mandal's central research laboratory, Belgaum and Hanagal Shri Kumareshwar college of pharmacy for providing all the needed facilities to perform the study.

Author contributions: Concept-L.V., Y.S; Design–L.V., Y.S; Supervision-L.V., Y.S; Resources – P.Y; Materials – P.V., L.S; Data Collection/or Processing – P.Y., L.V., Y.S; Analysis and /or Interpretation – L.V., Y.S., A.G., A.D; Literature search – P.Y., A.D., S.S; Writing- A.D., A.G., L.V., P.Y; Critical Reviews- L.S., S.S., P.Y.

Conflict of interest statement: The authors declare no conflict of interest.

REFERENCES

1. Hassan W, Kazmi SZ, Noreen H, Riaz A, Zaman B, 2016. Antimicrobial activity of *cinnamomum tamala* leaves. J nutr disord ther. 6(2), 2161-0509.[CrossRef]
2. Tamala AA. Ishan Dubey, Dr. Ritu M Gilhotra, Dr. Manmeet Singh saluja. The Int J Analytical Exp Modal Analysis. 2020; 9(7), 1657-71. [CrossRef]
3. Mann JR, DuBois RN. Cancer chemoprevention: myth or reality? Drug Discov Today Ther Strateg. 2004; 1(4),403-9.[CrossRef]
4. Seigneuric R, Markey L, SA Nuyten D, Dubernet C, TA Evelo C, Finot E, Garrido C. From nanotechnology to nanomedicine: applications to cancer research. Curr Mol Med. 2010;10(7), 640-52. [CrossRef]
5. Novelles MC, Brown TS, Feliciano DN. Silver nanoparticles as proapoptotic drugs: pharmacological basis in non-metastatic skin melanoma. Pharm Pharmacol Int J. 2022;10(3), 66-74. [CrossRef]
6. Ramasamy K, Shanmugam M, Balupillai A, Govindhasamy K, Gunaseelan S, Muthusamy G, Robert BM, Nagarajan RP. Ultraviolet radiation-induced carcinogenesis: Mechanisms and experimental models. J Radiat Res. 2017; 8(1), 4. [CrossRef]
7. Nadaroglu H, Gungor AA, Selvi IN. Synthesis of nanoparticles by green synthesis method. *Int J* Innov Res Rev. 2017; 1(1),6-9. [CrossRef]
8. Sarkar S, Kotteeswaran V. Green synthesis of silver nanoparticles from aqueous leaf extract of Pomegranate (*Punica granatum*) and their anticancer activity on human cervical cancer cells. Adv Nat Sci Nanosci Nanotechnol. 2018; 9(2),1-10 . [CrossRef]

9. Krishnan V, Bupesh G, Manikandan E, Thanigai AK, Magesh S, Kalyanaraman R, Maaza M. Green synthesis of silver nanoparticles using *Piper nigrum* concoction and its anticancer activity against MCF-7 and Hep-2 cell lines. J Antimicro. 2016; 2: 2472- 1212.[CrossRef]
10. Venkatesan B, Subramanian V, Tumala A, Vellaichamy E. Rapid synthesis of biocompatible silver nanoparticles using aqueous extract of *Rosa damascena* petals and evaluation of their anticancer activity. Asian Pac J Trop Med. 2014; 7:294-300. [CrossRef]
11. Lakshmanan G, Sathiyaseelan A, Kalaichelvan PT, Murugesan K. Plant-mediated synthesis of silver nanoparticles using fruit extract of *Cleome viscosa* L.: assessment of their antibacterial and anticancer activity.Karbala Int J Mod Sci. 2018; 4(1),61-8. [CrossRef]
12. Shahwar D, Ullaha S, Khan MA, Ahmad N, Saeed A, Ullah S. Anticancer activity of *Cinnamon tamala* leaf constituents towards human ovarian cancer cells. Pak J Pharm Sci. 2015; 28(3). [CrossRef]
13. Dumbre RK, Kamble MB, Patil VR. Inhibitory effects by ayurvedic plants on prostate enlargement induced in rats. Pharmacogn Res. 2014; 6(2),127.[CrossRef]
14. Kushwaha RK, Deepa HN, Karkera P, Jayashree S. Antibacterial Activity of Silver Nanoparticles Synthesized Using *Syzygium aromaticum*, *Cinnamomum tamala*,*Cinnamomum cassia* Plant Extract. J Pharm Res Int. 2021; 20-31. [CrossRef]
15. Dash SS, Samanta S, Dey S, Giri B, Dash SK. Rapid green synthesis of biogenic silver nanoparticles using *Cinnamomum tamala* leaf extract and its potential antimicrobial application against clinically isolated multidrug-resistant bacterial strains. Biol Trace Elem. 2020; Res, 198(2),681-96. [CrossRef]
16. Mir SR, Ali M, Kapoor R. Chemical composition of essential oil of *Cinnamomum tamala* Nees et Eberm. leaves. Flavour Fragr J. 2004; 19(2), 112-4. [CrossRef]
17. Vijapur LS, Hiremath JN, Bonageri NN, Desai AR. *Murraya koenigii*: biogenic synthesis of silver nanoparticles and their cytotoxic effects against MDA-MB-231, human breast cancer cell lines. World J Pharm Med Res. 2019; 5(6): 206-11. [CrossRef]
18. Jaast S, Grewal A. Green synthesis of silver nanoparticles, characterization and evaluation of their photocatalytic dye degradation activity. Curr Opin Green Susta Chem. 2021; 4:1-6. [CrossRef]
19. Meva FE, Segnou ML, Ebongue CO, Ntoumba AA, Kedi PB, Deli V, Etoh MA, Mpondo EM. Spectroscopic synthetic optimizations monitoring of silver nanoparticles formation from *Megaphrynium macrostachyum* leaf extract. Rev bras farmacogn. 2016; 26(5), 640-6. [CrossRef]
20. Vijapur LS, Srinivas Y, Desai AR, Hiremath JN, Swami CI, Shidramshettar SL. Antimicrobial activity of the biosynthesized silver nanoparticles of *Gossypium hirsutum* leaves extract. *GSC* biol. pharm. sci. 2021;15(3),189-98. [CrossRef]
21. Elamawi RM, Al-Harbi RE, Hendi AA. Biosynthesis and characterization of silver nanoparticles using *Trichoderma longibrachiatum* and their effect on phytopathogenic fungi. Egypt J Biol Pest Co. 2018; 28(1), 1-1.[CrossRef]
22. Anandalakshmi K, Venugobal J, Ramasamy V. Characterization of silver nanoparticles by green synthesis method using *Pedalium murex* leaf extract and their antibacterial activity. Appl Nanosci. 2016; (3),399-408. [CrossRef]
23. Yadav M, Yadav A, Yadav JP. In vitro antioxidant activity and total phenolic content of endophytic fungi isolated from Eugenia jambolana Lam. Asian Pac J Trop Med. 2014; 7, 256-61. [CrossRef]
24. Wang L, Hu C, Shao L. The antimicrobial activity of nanoparticles: present situation and prospects for the future. Int. J. Nanomed. 2017;12:1227-1249.[CrossRef]
25. Khandelwal K. Practical Pharmacognosy.20th ed. Nirali prakashan.2010; 25.1-25.9. [CrossRef]
26. Ahmed S, Saifullah, Ahmad M, Swami BL, Ikram S. Green synthesis of silver nanoparticles using Azadirachta indica aqueous leaf extract. J Radiat Res Appl Sci. 2016; 9(1), 1-7. [CrossRef]
27. Devaraj P, Kumari P, Aarti C, Renganathan A. Synthesis and characterization of silver nanoparticles using cannonball leaves and their cytotoxic activity against MCF-7 cell line. J Nanotechnol. 2013;1-5. [CrossRef]
28. Antimicrobial susceptibility testing protocols. Schwalve, Moore and Goodwin, Crc Press 2007.
29. MTT Cell Proliferation Assay Instruction Guide – ATCC, VA, USA http://www.atcc.org
30. Kumbar VM, Peram MR, Kugaji MS, Shah T, Patil SP, Muddapur UM, Bhat KG. Effect of curcumin on growth, biofilm formation and virulence factor gene expression of Porphyromonas gingivalis. Odontology. 2021; 109(1), 18-28. [CrossRef]
31. Peram MR, Jalalpure S, Kumbar V, Patil S, Joshi S, Bhat K, Diwan P. Factorial design based curcumin ethosomal nanocarriers for the skin cancer delivery: in vitro evaluation. J Liposome Res. 2019; 29(3), 291-311. [CrossRef]

32. Bin-Jumah M, Monera AA, Albasher G, Alarifi S. Effects of green silver nanoparticles on apoptosis and oxidative stress in normal and cancerous human hepatic cells in vitro. Int J Nanomedicine. 2020; 15, 1537-1548. [CrossRef]